NANO LETTERS
Cite This: Nano Lett. XXXX, XXX, XXX−XXX
Letter
pubs.acs.org/NanoLett

All-Mechanical Polarization Control and Anomalous (Electro)Mechanical Responses in Ferroelectric Nanowires

D. Pappas, Z. G. Fthenakis, and I. Ponomareva*

Department of Physics, University of South Florida, Tampa, Florida 33620, United States

ABSTRACT: Piezoelectric and ferroelectric nanowires exhibit properties and phases that are not available in the bulk. They are extremely promising for functional nanoscale application. On the basis of atomistic first-principles-based simulations, we predict an all-mechanical polarization control in ferroelectric nanowires. We report that the application of uniaxial compressive stress to ferroelectric nanowires with poor surface charge compensation leads to a reversible phase switching between the polar phase with axial polarization and macroscopically nonpolar flux-closure phase. The phase switching is associated with anomalously large changes in polarization and piezoelectric and mechanical response. In particular, in $PbTiO_3$ nanowires the values as large as 5400 pC/N and 140 TPa^{-1} are predicted for the piezoelectric coefficient and elastic constant, respectively. Remarkably, the effect persists up to the gigahertz frequency which is potentially promising for nanoscale applications, such as nanogenerators, biomedical electronics, monitoring devices, nanosensors, nanotransducers, and nanoactuators.

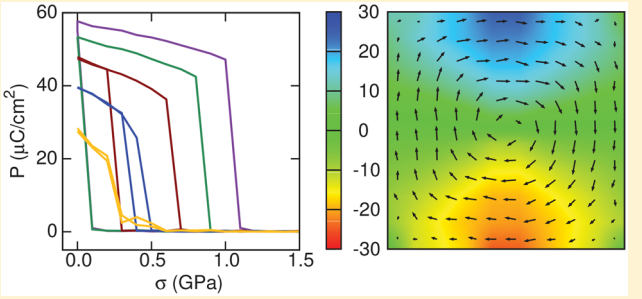

KEYWORDS: *Phase switching, electromechanical response, ferroelectric nanowires, molecular dynamics*

Piezoelectric and ferroelectric nanowires are promising candidates for nanoscale functional applications,[1−10] including biomedical electronics,[11] self-powered wearable and human activity monitoring devices,[12] and multienergy harvesting.[13] For example, piezoelectric zinc-oxide nanowires were found to function as nanogenerators for self-powered nanodevices[1−4] where they can produce the output current of 0.6 μA and associated current density of 20 $\mu A/cm^2$,[1] while sodium−potassium niobate nanorods were reported to have the short-circuit current of 5.0 μA.[5] $KNbO_3$ nanowire composite structures were reported to function as flexible pyroelectric nanogenerators,[6] while ferroelectric PZT nanowires were found to exhibit dramatically high pyroelectric open-circuit voltage and short-circuit current in a pyroelectric nanogenerator.[8] P3HT/ZnO micro/nanowire heterojunctions were proposed as functional elements for solar cells.[7] Textured ZnO nanowire film was developed for simultaneous or independent harvesting of mechanical and biochemical energy.[14] Piezoelectric and ferroelectric nanowires often exhibit properties that are not accessible in bulk. Some examples include anomalous coupling of light into the ferroelectric nanowire,[15] enhanced Curie temperature,[16] hardening of the soft modes,[17] enhanced energy conversion and storage,[18] unusual phase transitions,[19] phases,[20] and morphotropic phase boundary.[21]

Interestingly, the unusual morphotropic phase boundary in $Pb(Zr_{0.5}Ti_{0.5})O_3$ nanowires was predicted to exhibit outstanding values of piezoelectric coefficient d_{31} (up to 4900 pC/N) and of dielectric susceptibility (up to 40 000).[21] This phase boundary is associated with a transition from a polar to a vortex phase under the application of modulated electric field with the magnitude 0.4 V/nm. However, application of such modulated high-magnitude electric field is rather challenging which explains the delay in experimental demonstration of this boundary. On the other hand, the possibility to switch between the vortex and ferroelectric phases by application of electric field concomitant with order-of-magnitude changes in piezoelectric and nonlinear optical responses was experimentally demonstrated in oxide superlattices.[22] Theoretically, large piezoelectric (up to 1500 pC/N) and piezotoroidal (up to 0.4 e/GPa Å in magnitude) responses were predicted in $BaTiO_3$/$SrTiO_3$ composite nanowires from first-principles-derived simulations,[23] whereas the feasibility of vortex states switching by stress was predicted in ref 24 on the basis of phase-field simulations. Strain-induced vortex-to-uniform polarization transitions were predicted in $PbSr_2Ti_2O_7$ patterned disks using microscopic Landau−Ginzburg−Devonshire free energy functional theory.[25] At the same time, the possibility to induce polar to nonpolar vortex-like phase switching in nanowires by application of external stress has been so far overlooked. In ref 17 it was predicted that $PbTiO_3$ nanowires with poor surface charge compensation develop a flux-closure (FC) phase (or vortex-like phase) in the presence of uniaxial compressive stress, while stress-free nanowires exhibit a polar (P) phase with axial polarization direction, which points to the potential of such nanowires to switch phases. The aims of this work are (i) to predict the possibility to reversibly switch between the P

Received: July 10, 2018
Revised: August 3, 2018
Published: August 8, 2018

DOI: 10.1021/acs.nanolett.8b02818
Nano Lett. XXXX, XXX, XXX−XXX

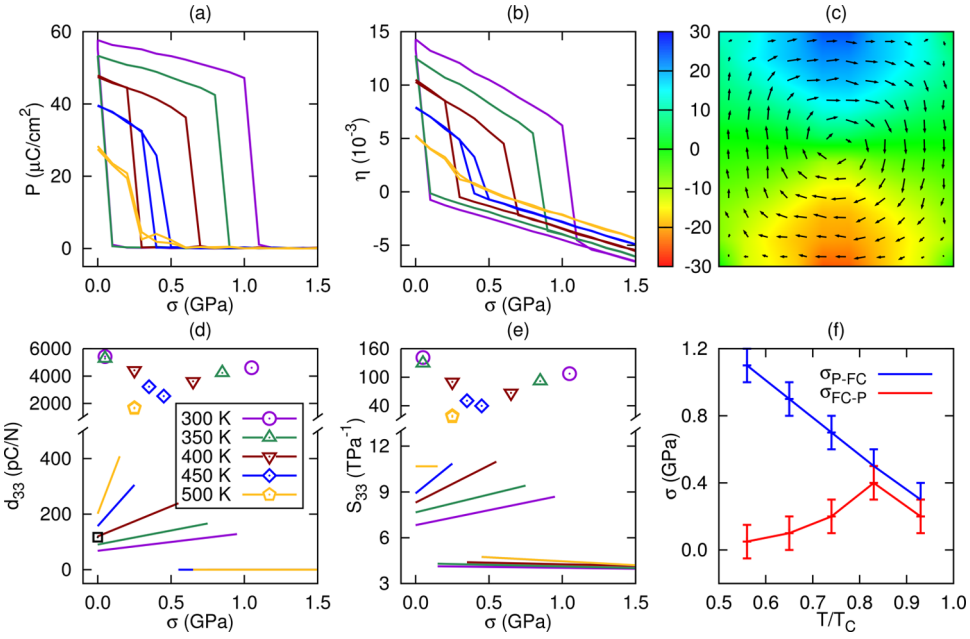

Figure 1. Dependence of the polarization P (a), strain component η (b), piezoelectric coefficient d_{33} (d), and elastic constant s_{33} (e) on stress applied in quasi-static regime. Symbol "□" in panel (d) gives the experimental value[37] for d_{33}. (c) Schematic visualization of the dipole pattern in the nanowire's cross section for σ = 2.0 GPa. The color box gives the values of the projection of the local polarization onto the x-axis in μC/cm^2. The legend of panel (d) applies to panels (a), (b), and (e) as well. (f) Dependence of the σ_{P-FC} and σ_{FC-P} stresses on the fractional temperature T/T_C. The error bar indicates the stress step used in simulations.

and nonpolar FC phases in $PbTiO_3$ nanowires by application of uniaxial compression; (ii) to report the anomalous electromechanical and mechanical responses associated with such stress-driven transformation; (iii) to explore the high-frequency dynamics of this stress-driven phase switching; and (iv) to discuss the potential applications of this phenomenon in nanogenerators and other nanodevices.

To reach our aims we used a first-principles-based atomistic approach to simulate $PbTiO_3$ nanowire with a square cross section of 4.8 nm lateral size grown along the [001] pseudocubic direction. Such a model represents ultrathin perovskite nanowires grown experimentally.[26−29] For example, $PbTiO_3$ nanowires with square cross section and diameters ranging from 20 to 500 nm were synthesized in the work by Wang et al.,[29] while 35−400 nm square cross section $PbTiO_3$ nanorods were reported in ref 30. Single crystalline $BaTiO_3$ nanowires with a principle axis along the nanowire length and diameters ranging from 3 to 100 nm have been reported.[27] The nanowire is modeled by a 12 × 12 × 12 supercell periodic along the axial direction (z Cartesian axis in our case) to simulate infinitely long nanowire. The energy of the supercell is given by the effective Hamiltonian of ref 31. The degrees of freedom for the Hamiltonian include local soft modes, $\mathbf{u}_i$, and local strain variables, η_i, expressed in Voigt notation. The local soft modes are proportional to the dipole moment, $\mathbf{d}_i = Z^*\mathbf{u}_i$, in the unit cell i, where Z^* is the Born effective charge. The local strain variables describe deformations at the level of the unit cell and are taken to be the sum of homogeneous and inhomogeneous strain variables. In these variables, the effective Hamiltonian is

$$E^{tot} = E^{self}(\{\mathbf{u}_i\}) + E^{dpl}(\{\mathbf{u}_i\}) + E^{short}(\{\mathbf{u}_i\}) + E^{elas}(\{\eta_i\}) + E^{int}(\{\mathbf{u}_i\}, \{\eta_i\}) + \sigma_j\eta_j^{hom} + \beta Z^* \sum_i \langle \mathbf{E}_{dep}\rangle \cdot \mathbf{u}_i \quad (1)$$

The first term describes the energy of the isolated local modes relative to that of the perfect cubic structure. The second term provides long-range dipole−dipole interaction between the local modes belonging to different unit cells. Note that for simulations of long-range dipole−dipole interactions in the nanowire we use the computational approach for nanostructures[32] which allows application of periodic boundary conditions along the nanowire's axial direction only. The third term gives the energy of short-range interactions (up to the third nearest neighbors) between the local modes. $E^{elas}(\{\boldsymbol{\eta}_i\})$ is the elastic energy associated with both unit cell and supercell deformations, while the $E^{int}(\{\mathbf{u}_i\},\{\boldsymbol{\eta}_i\})$ describes the interaction between the local modes and the local strains, which is critical for an accurate description of ferroelectric phase transitions. The sixth term in eq 1 describes the interaction of the homogeneous strain variables, η^{hom}, with the external stress, given by a stress tensor σ_j. The summation over the repeated indices is assumed. Note that for convenience of presentation we assign positive sign to compression which explains the positive sign in front of the term. The last term describes screening of the surface charge that is achieved by the application of a homogeneous electric field, $\langle \mathbf{E}_{dep}\rangle$, that opposes the depolarizing field. The strength of the field is controlled by the parameter β that gives the fraction of the screening field with respect to the maximum depolarizing field that can exist in the nanowire. In particular, β = 1 describes ideal short-circuit boundary conditions, while β = 0 describes ideal open-circuit boundary conditions. All the interaction parameters are derived from first-principles calculations.[31]

DOI: 10.1021/acs.nanolett.8b02818
Nano Lett. XXXX, XXX, XXX−XXX

Such Hamiltonian reproduces correctly both the static and dynamical properties of $PbTiO_3$.[31]. In particular, it correctly predicts a single phase transition from the paraelectric cubic to the ferroelectric tetragonal phase at 600 K in bulk $PbTiO_3$, which compares well with the experimental Curie point of 763 K. Moreover, the Hamiltonian reproduces 0 K soft mode frequencies obtained from first-principles simulations as well as the experimental data at finite temperatures.[31] Here the Hamiltonian is used in the framework of classical molecular dynamics (MD) to study both equilibrium and dynamical properties of the nanowire.

To obtain equilibrium structures, we use the simulated annealing technique in which the simulated sample is slowly annealed from 800 K down to 10 K in steps of 10 K. For each temperature we use 40 000 MD steps (40 ps of total simulation time) to equilibrate the supercell. The temperature is controlled by Evans−Hoover thermostat.[33] In this work we simulate nanowire under realistic open-circuit boundary conditions which is achieved by screening 10% of the surface charge ($\beta = 0.1$). Such conditions are known to result in the polarization aligned along the nanowire's axis[34] which occurs most often in experimental settings.[28] Note that for this study the exact percentage of the surface charge compensation is not important as long as it confines the polarization to the axial direction and can range from 0 to 85%.[34] We also carried out some simulations for bulk which was modeled by $12 \times 12 \times 12$ supercell periodic along all three Cartesian directions. To investigate the nanowire's response to external stress, we apply a uniaxial stress along the nanowire's growth direction. Note that experimentally uniaxial stress up to 0.2 GPa has been used to control magnetic skyrmions.[35] Two regimes are considered: quasi-static and high-frequency dynamics. In the first regime the uniaxial stress is applied under quasi-equilibrium conditions which is technically carried out using MD. In such simulations the uniaxial stress is first increased from 0.0 to 2.0 GPa in increments of 0.1 GPa. For each value of stress we used 100 000 MD steps. After the maximum stress value is reached the stress is slowly decreased to zero in decreaments of 0.1 GPa. For the high-frequency regime the stress is applied dynamically as follows: $\sigma = \sigma_0(1 - \cos \omega t)$, where σ_0 is the magnitude of the uniaxial stress, which was set to 1.0 GPa. We simulated frequencies 500, 1500, 5000, and 5500 MHz, which are within the range of practical importance.[36] Both quasi-static and high-frequency simulations were carried out for temperatures 300, 350, 400, 450, and 500 K, which are technologically relevant.

From annealing simulations we found that under chosen electrical boundary conditions the nanowire develops the polarization along the axial direction below the computational Curie temperature of 540 K which is in agreement with the previous studies.[17,28,34] The direction of polarization is confined to the axial direction in this case due to a large depolarizing field associated with other polarization directions. We begin by considering evolution of the axial polarization and strain under quasi-static application of the uniaxial stress. Our data for different temperatures are given in Figure 1(a) and (b). Interestingly, we find that for all temperatures considered as the stress increases the net polarization disappears at some critical value of stress. The component of the strain tensor that describes the axial deformation experiences a discontinuity at the same critical stress value. For example, for $T = 300$ K the critical value of the stress is 1.1 ± 0.1 GPa. These abrupt changes in the order parameters point to a phase transformation at the critical stress value. Inspection of the dipole patterns reveals that the phase transformation is associated with formation of an FC pattern which is shown in Figure 1(c). The formation of this phase is a compromise between the electromechanical coupling that favors transverse polarization direction under the axial compressive stress and the depolarizing energy that disfavors such direction. During the phase switching the axial strain changes from positive in the polar phase to negative in the FC phase [see Figure 1(b)]. The most remarkable feature is that as the stress is released the nanowire transforms back into the macroscopically polar phase with axial polarization direction in all cases considered. The critical stress associated with P−FC phase switching is labeled as σ_{P-FC}, while the critical stress associated with a reverse FC−P phase is labeled as σ_{FC-P}. Interestingly, at the critical stress values the discontinuity in the polarization and strain are expected to result in anomalous values of piezoelectric coefficient $d_{33} = dP/d\sigma$ and elastic constant $s_{33} = d\eta/d\sigma$, respectively. To estimate the anomalous values we compute the derivatives using the finite-differences approach, $d_{33} \approx \Delta P/\Delta\sigma$ and $s_{33} \approx \Delta\eta/\Delta\sigma$, while the coefficients away from the critical stresses are computed analytically using a quadratic fit to the computational $P(\sigma)$ and $\eta(\sigma)$. The latter ones compare well with experimental values for $PbTiO_3$ and are reported in the lower part of Figure 1(d). Anomalous values are an order of magnitude higher and reported in the upper parts of Figure 1(d). Remarkably, at the critical value of the stress for $T = 300$ K, the piezoelectric coefficient d_{33} reaches the value of $d_{33} \approx 5400$ pC/N, while the elastic constant s_{33} reaches the value of $s_{33} \approx 140$ TPa^{-1}. For comparison the best available values for d_{33} are 3200 pC/N in PMN−PT, while the best values of s_{33} are 141 TPa^{-1}.[36] Given that our values were obtained using the computational stress step $\Delta\sigma = 0.1$ GPa, they are likely to underestimate the true values. In fact, our computational results suggest that at the point of the phase switching the discontinuous changes in the polarization and strain are likely to lead to the divergence of both coefficients. Note that the same FC phase was reported as the equilibrium phase of the nanowire under the uniaxial compression.[17]

Thus, our simulations predict that the response of the nanowire to the applied stress is qualitatively different from bulk as the latter does not develop FC phases. To further investigate, we carried out similar computations for bulk $PbTiO_3$. In such calculations the stress was applied along the polar direction. We found that at the critical value of stress the polarization rotates toward one of the [001] directions that is not associated with the applied stress. There exist two critical differences between the response to the uniaxial stress applied along the polar direction in bulk and nanowire with poor surface charge compensation. The first difference is that the high-stress phase in the nanowire is macroscopically nonpolar, while the high-stress phase in the bulk is macroscopically polar. The second difference is that after the stress is released in bulk no further phase switching occurs, and the simulated sample remains polarized along the same direction as in the stressed sample as the three [001] directions are degenerate in the absence of stress. In other words, in bulk, the stress-driven phase switching is irreversible. The nanowire, on the contrary, returns to the original polar phase with the axial polarization direction after the stress is released. In general, the ability to turn off ferroelectric response via conversion to the nonpolar phase is highly desirable as it allows for large tunability and susceptibilities.[22] Moreover, all-mechanical control of the

DOI: 10.1021/acs.nanolett.8b02818
Nano Lett. XXXX, XXX, XXX−XXX

ferroelectric phase is particularly attractive as it allows for superior electromechanical conversion and therefore opens a path to efficient energy harvesting in nanogenerators, mechanically operated logic, ultrasensitive nanoscale stress sensors, nanotransducers, nanoactuators, and others. It is important to mention that the behavior reported for the $PbTiO_3$ nanowire is not limited to individual nanowires but is expected to occur also in the nanowire arrays which are especially promising for nanogenerators.[1,9] Moreover, such arrays could even have an enhanced functionality as compared to individual nanowires. Indeed, the critical value of the stress is expected to depend on the nanowire size. In the arrays of nanowires the diameters of individual nanowires vary which is expected to lead to variations in the critical values of stress and, therefore, to an enhanced response for a wider range of stresses.

At 300 K we find a large hysteresis in the dependence of the polarization and strain on stress (see Figure 1(a) and (b)) which is a consequence of the energy barrier that exists between the P and FC phases. However, as the temperature increases and approaches the computational Curie point, T_C, the hysteresis drastically decreases. In fact, for 500 K we do not find any hysteresis. This is similar to the case of electric hysteresis in ferroelectrics that disappears on approaching the Curie point. Figure 1(f) shows the dependence of the critical stress for both P−FC and FC−P phase switching. We can see that as the temperature increases the critical stresses first merge with each other within our computational resolution and then begin to decrease as the transition temperature approaches owing to the decrease in the spontaneous polarization and associated decrease in the energy barrier between the polar and FC phases. At $T/T_C = 0.93$ the critical stress is 0.2 GPa which is accessible for experimental demonstrations and promising for potential applications. Indeed, uniaxial stresses of up to 0.2 GPa were used to control magnetic skyrmions.[35]

Next we look into the dynamics of this unusual response to the axial stress. For that, the simulations were carried out under periodic stress as described previously. The representative time evolution of the axial polarization and associated strain component at different temperatures are given in Figure 2. The data correspond to stress with frequency of 500 MHz. The responses to the stress field with other investigated frequencies are very similar. Our simulations reveal that the effect persists even at these high frequencies. Indeed, we observe the P−FC−P phase switching in all cases. Notice that both directions of the axial polarization appear in simulations. At the same time, we notice that at 300 K the polar phase fails to form for some periods [see Figure 2(a)]. Inspection of the dipole patterns for these cases reveals the formation of nonequilibrium phase with nanostripes when the stress is released. In such stripes the polarization aligns along either positive or negative z-direction. Similar effects were found for other frequencies at 300 K as well as for temperature of 350 K. On the other hand, such nonequilibrium phases no longer appear for temperatures 400 K and above as evident from Figure 2(c) and (e). For these temperatures we find that the nanowire always return to the polar phase with axial polarization as the stress is released. The associated time evolution of strain is given in Figure 2(b), (d), and (f). We find that the strain oscillates in phase with the polarization between rather large positive and negative values in all cases. The phase switching occurs through gradual polarization rotation from the axial direction to the direction in the FC phase and then back to the axial direction.

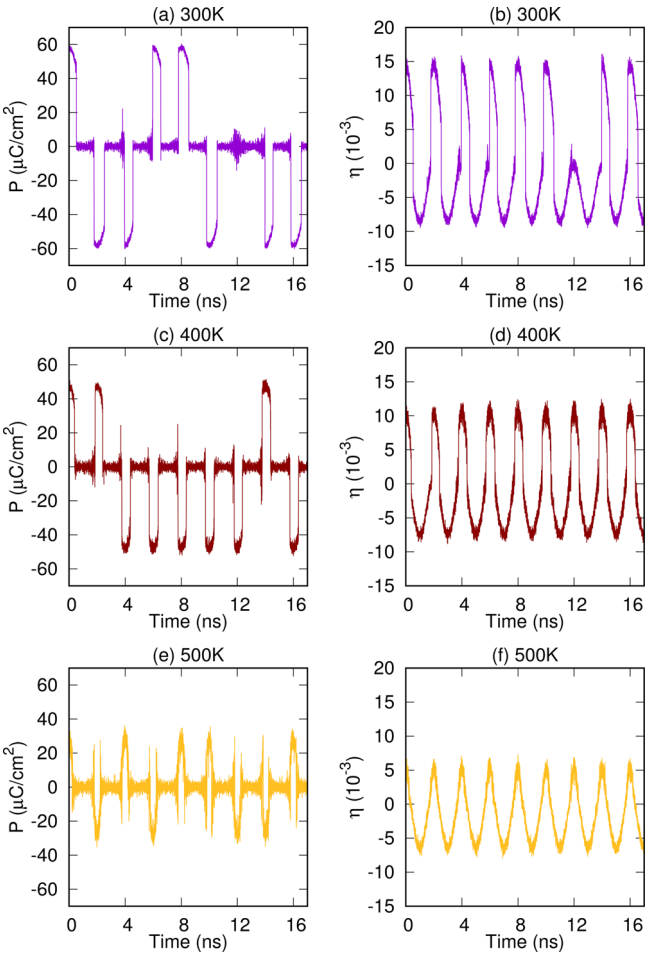

Figure 2. Time evolution of axial polarization (a), (c), and (e) and strain (b), (d), and (f) under dynamically applied stress with frequency 500 MHz. Temperatures are given in the titles.

To gain further insight into the dynamics of the effect, we plot the dependence of the average polarization and strain on the stress from these dynamical calculations in Figure 3. The average is taken over 9 periods. We also added data from quasi-static calculations for the purpose of comparison. At 300 K we find very pronounced dynamical effects. The average polarization in the polar phase under dynamical stress is significantly smaller than in the case of static calculations due to the aforementioned failure to develop axial polarization during some periods. The critical stress for the P−FC phase switching is larger in dynamical simulations which results in a larger hysteresis. For the strain response the difference between the quasi-static and dynamical stress application is mostly limited to the aforementioned differences in σ_{P-FC} and associated hysteresis. The data for 400 K are given in Figure 3(c) and (d). Here we find the differences in both σ_{P-FC} and σ_{FC-P} for the highest frequency. However, for frequency of 500 MHz these differences mostly disappear indicating the nearly quasi-equilibrium process. For 500 K [see Figure 3(e) and (f)] we find no significant differences between the quasi-static and dynamic cases. We have also computed d_{33} and s_{33} coefficients from the dynamical simulations by taking the numerical derivative of $\langle P\rangle(\sigma)$ and $\langle \eta\rangle(\sigma)$. At 300 K and for 500 MHz we found that d_{33} reaches the value of 3200 pC/N near P−FC phase switching and of 5000 pC/N near FC−P phase switching. Similarly, for the same settings we find s_{33} to

DOI: 10.1021/acs.nanolett.8b02818
Nano Lett. XXXX, XXX, XXX−XXX

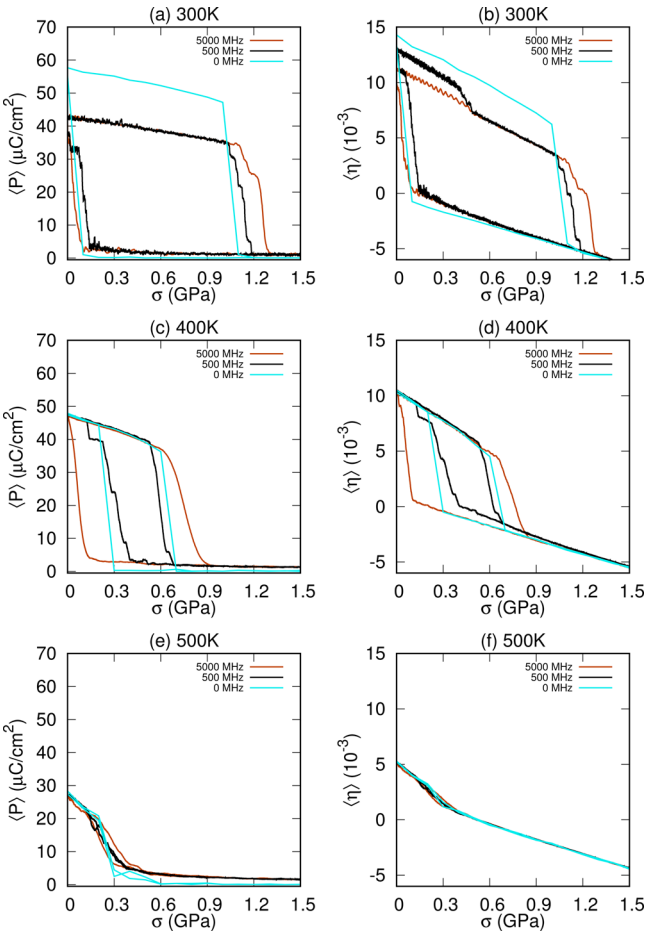

Figure 3. Dependence of axial polarization (a), (c), and (d) and of axial strain (b), (d), and (f) on stress applied dynamically. The frequency is indicated in the legend. For comparison we also included the dependencies from the quasi-static simulations.

reach values up to 76 and 160 TPa^{-1} for P−FC and FC−P phase switching, respectively.

It is important to establish whether the predicted anomalous behavior is unique to the nanowire studied in this work or a general property of ferroelectric nanowires. Let us first recall that the P−FC−P phase switching occurs as a consequence of energy competition between the depolarizing energy and electromechanical coupling orchestrated by the nanowire's shape/geometry. Therefore, we would expect this shape effect to occur in all ferroelectric nanowires with poor surface charge compensation. To confirm this we carried out additional quasi-static simulations in which we changed the size and the material of the nanowire. More specifically, we considered $PbTiO_3$ nanowires of larger lateral size of 6.2, 11.7, and 15.6 nm and also the lead-free $BaTiO_3$ nanowire with the lateral size of 4.8 nm. Note that $BaTiO_3$ nanowires exhibit a phase transition sequence[19,38] that is quite different from the case of $PbTiO_3$. In all cases we found that the reported anomalous behavior persists. This confirms that the predicted phase switching and the unusual behavior are a shape property.

In summary, we have used atomistic first-principles-based simulations to predict a possibility to control the polarization in ferroelectric nanowires with poor surface charge compensation by the application of uniaxial compression. Our simulations indicate that the uniaxial compression causes the nanowire to switch from the P phase with axial polarization into the macroscopically nonpolar FC phase. The unique feature of this phase switching is its reversibility: the nanowire returns to its original P phase as the stress is released. The effect is orchestrated by the competition between the electromechanical and depolarizing energy and, therefore, is prohibited in bulk. Furthermore, this peculiar effect is a shape property and, therefore, is expected to occur in ferroelectric nanowires only. At the point of the phase switching the nanowire is predicted to exhibit anomalous values of piezoelectric coefficient and elastic constant which in $PbTiO_3$ nanowire could reach 5400 pC/N and 140 TPa^{-1}, respectively. The all-mechanical control of polarization and associated anomalous (electro)mechanical properties could potentially lead to superior performance in nanoscale devices, such as nanogenerators, nanoactuators, nanosensors, nanotransducers, nanoscale memories, and others.

AUTHOR INFORMATION

Corresponding Author

*E-mail: iponomar@usf.edu.

ORCID

I. Ponomareva: 0000-0001-8937-4401

Notes

The authors declare no competing financial interest.

ACKNOWLEDGMENTS

The present work is supported by the U.S. Department of Energy, Office of Basic Energy Sciences, Division of Materials Sciences and Engineering under grant DE-SC0005245. Some computer time was provided by USF Research Computing, sponsored in part by National Science Foundation MRI CHE-1531590.

REFERENCES

(1) Song, J.; Wang, Z. L.; Wang, X.; Liu, J.; Gao, Y. *IEEE Perv. Comput.* **2008**, *7*, 49−55.
(2) Wang, Z. L.; Song, J. *Science* **2006**, *312*, 242−246.
(3) Gao, P.; Song, J.; Liu, J.; Wang, Z. *Adv. Mater.* **2007**, *19*, 67−72.
(4) Song, J.; Zhou, J.; Wang, Z. L. *Nano Lett.* **2006**, *6*, 1656−1662.
(5) Xu, H.; Lee, T.; Park, S.; Kim, B.; Nahm, S. *J. Am. Ceram. Soc.* **2017**, *100*, 1673−1681.
(6) Yang, Y.; Jung Jong, H.; Yun, B. K.; Zhang, F.; Pradel, K. C.; Guo, W.; Wang, Z. L. *Adv. Mater.* **2012**, *24*, 5357−5362.
(7) Yang, Y.; Guo, W.; Zhang, Y.; Ding, Y.; Wang, X.; Wang, Z. L. *Nano Lett.* **2011**, *11*, 4812−4817.
(8) Yang, Y.; Zhou, Y.; Wu, J. M.; Wang, Z. L. *ACS Nano* **2012**, *6*, 8456−8461.
(9) Zi, Y.; Wang, Z. L. *APL Mater.* **2017**, *5*, 074103.
(10) Herchig, R.; Schultz, K.; McCash, K.; Ponomareva, I. *Nanotechnology* **2013**, *24*, 045501.
(11) Zhang, G.; Li, M.; Li, H.; Wang, Q.; Jiang, S. *Energy Technol.* **2018**, *6*, 791−812.
(12) Chen, Y.; Zhang, Y.; Yuan, F.; Ding, F.; Schmidt, O. G. *Adv. Elect. Mater.* **2017**, *3*, 1600540.
(13) Wang, S.; Wang, Z. L.; Yang, Y. *Adv. Mater.* **2016**, *28*, 2881−2887.
(14) Pan, C.; Li, Z.; Guo, W.; Zhu, J.; Wang, Z. L. *Angew. Chem., Int. Ed.* **2011**, *50*, 11192−11196.
(15) Nah, S.; Kuo, Y.-H.; Chen, F.; Park, J.; Sinclair, R.; Lindenberg, A. M. *Nano Lett.* **2014**, *14*, 4322−4327.
(16) Datta, A.; SanchezJimenez, P. E.; Al Orabi Rabih, A. R.; Calahorra, Y.; Ou, C.; Sahonta, S.; Fornari, M.; KarNarayan, S. *Adv. Funct. Mater.* **2017**, *27*, 1701169.
(17) Herchig, R.; Ponomareva, I. *J. Appl. Phys.* **2017**, *122*, 214103.

DOI: 10.1021/acs.nanolett.8b02818
Nano Lett. XXXX, XXX, XXX−XXX

(18) Herchig, R.; Mani, B.; Lisenkov, S.; Ponomareva, I. *Comput. Mater. Sci.* **2016**, *117*, 468−471.
(19) Louis, L.; Gemeiner, P.; Ponomareva, I.; Bellaiche, L.; Geneste, G.; Ma, W.; Setter, N.; Dkhil, B. *Nano Lett.* **2010**, *10*, 1177−1183.
(20) Naumov, I. I.; Bellaiche, L.; Fu, H. *Nature* **2004**, *432*, 737.
(21) Fu, X.; Naumov, I. I.; Fu, H. *Nano Lett.* **2013**, *13*, 491−496.
(22) Damodaran, A. R.; et al. *Nat. Mater.* **2017**, *16*, 1003.
(23) Chen, W. J.; Zheng, Y.; Wang, B. *Sci. Rep.* **2015**, *5*, 11165.
(24) Yuan, S.; Chen, W.; Ma, L.; Ji, Y.; Xiong, W.; Liu, J.; Liu, Y.; Wang, B.; Zheng, Y. *Acta Mater.* **2018**, *148*, 330−343.
(25) Lee, B.; Nakhmanson, S. M.; Heinonen, O. *Appl. Phys. Lett.* **2014**, *104*, 262906.
(26) Gu, H.; Hu, Y.; You, J.; Hu, Z.; Yuan, Y.; Zhang, T. *J. Appl. Phys.* **2007**, *101*, 024319.
(27) Spanier, J. E.; Kolpak, A. M.; Urban, J. J.; Grinberg, I.; Ouyang, L.; Yun, W. S.; Rappe, A. M.; Park, H. *Nano Lett.* **2006**, *6*, 735−739.
(28) Buscaglia, V.; Teresa Buscaglia, M. *Nanoscale Ferroelectrics and Multiferroics*; John Wiley & Sons, Ltd., 2016; p 200.
(29) Wang, J.; Wylie-van Eerd, B.; Sluka, T.; Sandu, C.; Cantoni, M.; Wei, X.-K.; Kvasov, A.; McGilly, L. J.; Gemeiner, P.; Dkhil, B.; Tagantsev, A.; Trodahl, J.; Setter, N. *Nat. Mater.* **2015**, *14*, 985.
(30) Rorvik, P.; Almli, A.; T J van Helvoort, A.; Holmestad, R.; Tybell, T.; Grande, T.; Einarsrud, M.-A. *Nanotechnology* **2008**, *19*, 225605.
(31) Mani, B. K.; Chang, C.-M.; Ponomareva, I. *Phys. Rev. B: Condens. Matter Mater. Phys.* **2013**, *88*, 064306.
(32) Ponomareva, I.; Naumov, I. I.; Kornev, I.; Fu, H.; Bellaiche, L. *Phys. Rev. B: Condens. Matter Mater. Phys.* **2005**, *72*, 140102.
(33) Rapaport, D. *The art of Molecular Dynamics Simulation*; Cambridge University Press, 2001.
(34) Ponomareva, I.; Naumov, I. I.; Bellaiche, L. *Phys. Rev. B: Condens. Matter Mater. Phys.* **2005**, *72*, 214118.
(35) Nii, Y.; Nakajima, T.; Kikkawa, A.; Yamasaki, Y.; Ohishi, K.; Suzuki, J.; Taguchi, Y.; Arima, T.; Tokura, Y.; Iwasa, Y. *Nat. Commun.* **2015**, *6*, 8539.
(36) Ye, Z.-G., Ed. *Handbook of Advances dielectric, piezoelectric and ferroelectric materials: Synthesis, properties and applications*; Woodhead Publishing Limited, 2008.
(37) Newnham, R. E. *Properties of materials: Anisotropy, symmetry, structure*; Oxford University Press, 2004.
(38) Herchig, C.-M.; Chang, R.; Mani, B. K.; Ponomareva, I. *Sci. Rep.* **2015**, *5*, 17294.

DOI: 10.1021/acs.nanolett.8b02818
Nano Lett. XXXX, XXX, XXX−XXX